

Poly(ethylene succinate-co-lactic acid) as a Multifunctional Additive for Modulating the Miscibility, Crystallization, and Mechanical Properties of Poly(lactic acid)

Yinbiao Feng,[§] Cong Wang,[§] Junjiao Yang, Tianwei Tan, and Jing Yang*Cite This: *ACS Omega* 2024, 9, 6578–6587

Read Online

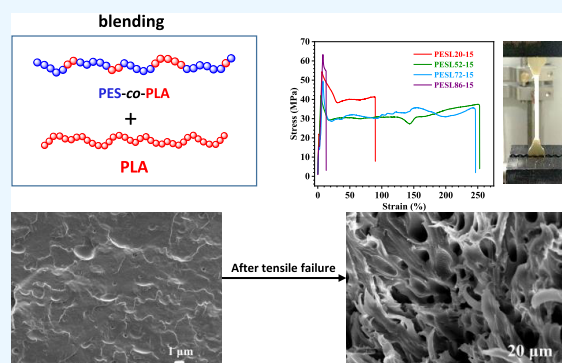
ACCESS |

Metrics & More

Article Recommendations

Supporting Information

ABSTRACT: Polymer blending offers an effective and economical approach to overcome the performance limitations of poly(lactic acid) (PLA). In this study, a series of copolymers poly(ethylene succinate-co-lactic acid) (PESL) were synthesized, featuring lactic acid (LA) contents that ranged from 20 to 86 wt %. This synthesis involved a one-pot industrial melt polycondensation process using succinic acid (SA), ethylene glycol (EG), and LA, catalyzed by titanium tetraisopropoxide (TTP). The goal was to produce a fully biobased copolymer expected to exhibit partial miscibility with pure poly(lactic acid) (PLA). To assess the capability of PESL copolymers in toughening PLA, we conducted tensile testing on PLA/PESL blends containing 15 wt % PESL. As a result, an elongation at break for the blends with 15 wt % loading of the copolymer PESL72 was directly enhanced to 250% with an ultimate strength of 35 MPa, compared to brittle PLA with less 10% tensile length. The morphological features of interfacial adhesion before and after tensile failure were measured by scanning electron microscopy (SEM). A significant enhancement in the chain mobility of the PLA/PESL blends was further evidenced by differential scanning calorimetry (DSC) and dynamic mechanical analysis (DMA). These findings hold promise for the development of functional packaging materials based on PLA. The proposed copolymer design, which boasts strong industrial feasibility, can serve as a valuable guide for enhancing the toughness of PLA.



1. INTRODUCTION

In the expansive realm of environmentally friendly polymers, poly(lactic acid) or polylactide (PLA) stands out as a noteworthy member.^{1–3} It belongs to the category of aliphatic polyesters and has been synthetically produced through chemocatalysis from renewable biogenic sources for several decades.^{4–7} PLA has garnered significant attention due to its blend of competitive mechanical strength, exceptional transparency, and commendable biodegradability in industrial settings.^{8–10} PLA is widely regarded as a sustainable alternative to petroleum-derived and nondegradable plastics, offering promising applications in various domains, particularly in the realm of disposable products.¹¹ These applications encompass eco-friendly packaging, tableware, water cups, and nursery items, all of which contribute to mitigating and addressing environmental concerns. However, it is important to note that PLA's mechanical performance inherently falls short of commonly used plastics like polyethylene (PE) and polyethylene terephthalate (PET). For instance, PLA exhibits extreme brittleness, with less than 10% elongation at breaking and relatively limited impact resistance.^{12,13} These deficiencies impose significant constraints on its utility in widespread industrial and medical applications where the material needs to undergo substantial plastic deformation under high-stress

levels.^{14,15} Therefore, the quest to enhance the toughness of PLA has remained a focal point of interest within both academic and industrial circles.^{16–18}

Numerous approaches and advanced technologies have been employed to enhance the toughness of PLA, such as the utilization of plasticizers, copolymerization with specific chemicals, and the introduction of reinforcing fillers.¹⁹ However, when compared, polymer blending emerges as an efficient and cost-effective strategy for rectifying the performance limitations of PLA while harnessing the unique advantages of a diverse array of existing polymers.²⁰ With a keen eye toward sustainable and eco-friendly development, researchers have successfully explored the blending of PLA with flexible, elastic, and biodegradable polyesters, including poly(butylene succinate) (PBS),²¹ poly(butylene adipate-co-terephthalate) (PBAT),²² and polycaprolactone (PCL).²³ This blending approach has yielded significant enhancements in

Received: September 27, 2023

Revised: November 4, 2023

Accepted: December 12, 2023

Published: February 1, 2024



toughness and tensile properties, thanks to the complementary characteristics of these materials. However, it is worth noting that despite achieving substantial improvements in elongation at break, the inherent challenge lies in the weak interfacial interactions between PLA and the incorporated toughening phase.^{24,25} This leads to a propensity for phase separation within the blended polymer system, ultimately resulting in some compromise in terms of strength and modulus properties.

In order to effectively address the immiscibility issues encountered in PLA-based biodegradable polymer blends, a range of compatibilization techniques has been employed to regulate the phase behavior and morphology of the blended materials. These techniques encompass the incorporation of premade block/graft copolymers that exhibit affinity for both phases,¹⁸ the utilization of reactive blending to form in situ copolymers,²⁶ the creation of cross-linked continuous networks,¹⁷ and the introduction of nanoparticles.¹⁹ However, when compared to the introduction of a third component aimed at reconciling polymer blending, a seemingly simpler and highly effective approach involves the use of copolymers containing lactic acid (LA) units to modify pure PLA through blending.²⁷ For instance, Ji et al. synthesized a series of monomethoxy poly(ethylene glycol)-PLA diblock copolymers with varying segment ratios and investigated their compatibility-enhancing effects in inherently immiscible PLA blends.²⁸ Additionally, Hakkarainen's research group developed a copolymer, poly(ethylene 2,5-furandicarboxylate)-*block*-polylactide, which was instrumental in tailoring interfacial properties and phase morphology.²⁹ This, in turn, contributed to significant improvements in the mechanical and other properties of PLA. One common characteristic shared by these blending materials is their origin as block copolymers produced through the ring-opening polymerization (ROP) of lactides in the presence of macroinitiators. To date, there have been limited reports regarding the use of random copolymerization of lactic acid with other polyesters for blending with PLA.

Poly(ethylene succinate) (PES), synthesized through the melt-copolymerization of biobased succinic acid (SA) and the commonly used chemical ethylene glycol (EG), represents a significant biodegradable polymer.^{30,31} PES stands out for its relatively high thermal degradation temperature and enhanced biodegradability compared with polybutylene succinate (PBS). Additionally, it boasts physical properties that are on par with certain conventional thermoplastics like linear low-density polyethylene and polypropylene.^{32–34} One of the notable advantages of PES is the ready availability and cost-effectiveness of its raw material, succinic acid (SA), which outperforms some emerging dicarboxylic acids in terms of affordability. PES also demonstrates commendable mechanical properties, and its melting temperature approaches approximately 100 °C. Although PES is commercially accessible, it has not yet reached production on a ton-scale.

Considering these advantageous characteristics, this study involves the synthesis of a series of poly(ethylene succinate)-*co*-poly(lactic acid) (PESL) copolymers with varying LA contents. This was achieved by adjusting the initial molar feed ratios of succinic acid (SA), ethylene glycol (EG), and lactic acid (LA) through a process of melt polycondensation. The resulting random copolymers exhibit impressive elongation at break, which complements the properties of PLA homopolymers. As the dual roles of compatibilizer and

modifier, the copolymers PESL with 15 wt % loading are anticipated to form physical blends with pure PLA. This research primarily focuses on analyzing the macrostructure and mechanical properties of these blended polymers. Additionally, a comprehensive exploration of the thermodynamic properties is conducted to gain insight into the performance of these PLA-based blends. It is worth noting that the raw materials used to synthesize the premade PESL copolymers are cost-effective and widely available. Furthermore, the melt polycondensation conditions employed are familiar within the realm of common polyesters such as PBS and PET. The biodegradable materials resulting from the blending of the copolymers PESL with PLA hold promising potential to meet the demand for disposable products, aligning with the growing need for eco-friendly solutions.

2. EXPERIMENTAL SECTION

2.1. Materials. Succinic acid (SA, 99.5%) was purchased from Tianjin Bailunsi Industrial Co., Ltd. Titanium tetraisopropoxide (TTP, $\geq 97\%$) was purchased from Alfa Aesar. 1,1,2,2-Tetrachloroethane (98%) was purchased from Aladdin. Lactic acid (L-LA, 95%) was purchased from Musashino Chemical (China) Co., Ltd. Commercial poly(lactic acid) (PLA, $M_n = 110$ kDa) was purchased from Nature Works Asia Pacific Co., Ltd. Trichloromethane, anhydrous methanol, and ethylene glycol (EG, $\geq 99\%$) were ordered from Beijing Chemical Works.

2.2. Synthesis of Copolymer PESL. SA (25 g, 0.212 mol), EG (13.8 g, 0.222 mol), LA with determined weight, and TTP (416.3 mg, 1.465 mmol) were added to the three-necked flask under a N_2 atmosphere. The esterification reaction was conducted at 190 °C for 4 h under a N_2 atmosphere. When the water was collected over 85% of the theoretical yield, the reaction temperature was increased to 210 °C, and polycondensation was performed at 20 Pa for 8 h. The resulting copolymers were dissolved in chloroform, precipitated with methyl alcohol, and dried under vacuum.

2.3. Preparation of PESL/PLA Blends. The copolymer PESL with a loading of 15 wt % and pure PLA were added to the Haake twin-screw compounder (Rheomix 600 p, Thermo Scientific Co., Germany). The temperature was set at 180 °C, and the rotational speed was 80 rpm for 10 min of blending. Then, the rotational speed was slowly adjusted to 3 rpm to obtain the blending materials.

2.4. Characterization Methods. The chemical structures of the obtained copolymers were characterized by 1H NMR recorded on a 500 MHz NMR instrument (Bruker Corporation, Germany) at 25 °C using $CDCl_3$ as solvent. GPC measurements of the copolymers were carried out on an Agilent LC 1260 instrument (Agilent Technologies Inc., California) equipped with a differential refractive index detector. A guard column and two 7.5 mm \times 300 mm PLgel MIXED-C columns were used. The measurements were performed using DMF as an eluent. Intrinsic viscosity was measured at 25 °C with an Ubbelohde viscometer. The IV value was determined from the extrapolated straight-line plot. The copolymers were dissolved in a mixed solution of phenol and 1,1,2,2-tetrachloroethane ($v/v = 1/1$).

Thermal stability properties were measured with thermogravimetric analysis (TGA) on a TA Q500 analyzer. The test was carried out at a rate of 10 °C/min from room temperature to 600 °C under a nitrogen atmosphere. Thermal properties were measured with differential scanning calorimetry (DSC)

Scheme 1. Synthesis Route of the Copolymer PESL via the Copolymerization of SA, EG, and LA

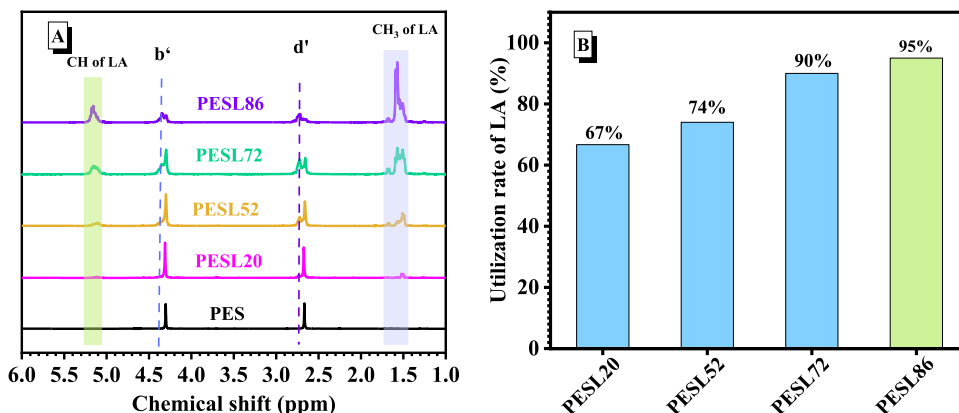
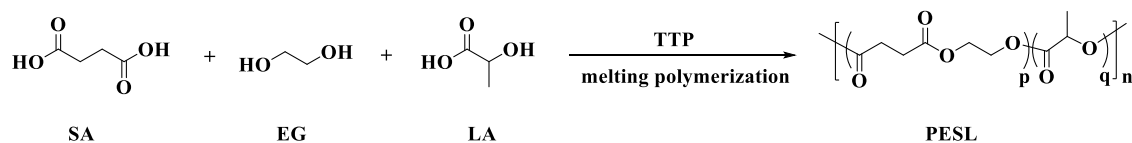


Figure 1. (A) Comparative ^1H NMR spectra of the copolymer PESL with various LA contents. (B) Utilization rate of LA during polycondensation.

on a TA-Q2000 thermal analyzer. The sample was first heated to 200 °C with a heating rate of 10 °C/min and then rapidly cooled to -70 °C with a rate of 180 °C/min and maintained at this temperature for 2 min. Then, the mixture was heated at a rate of 10 °C/min. Then, the sample was maintained at 150 °C for 2 min, followed by cooling down to 25 °C at the same rate.

Dynamic mechanical properties were measured with dynamic thermomechanical analysis (DMA) on a TA-Q800. Before measurement, rectangular strips were prepared with dimensions of 30 mm (length), 6 mm (width), and 2 mm (thickness), and then the test was carried out at a frequency of 3 Hz and heating rate of 5 °C/min from -80 to 100 °C.

Tensile tests were performed with dumbbell-shaped samples using a SUNS tensile testing machine with a 500 N load cell at a crosshead speed of 50 mm/min. The impact strength of the sample was measured using equipment electronic impact testing machine (Chengde Precision Testing Machine Corp., China; type number XJUD-5.5). The impact test was repeated at least five times for each sample, and the impact speed was 3.5 m/s.

The morphological observation was carried out using scanning electron microscopy (SEM) (UT-7800, Hitachi). The specimens used for observing phase morphology were prepared by cryofracturing the injection-molded blend samples in liquid nitrogen. Prior to SEM imaging, both the cryofractured and tensile failure surfaces were sputter-coated with gold.

Polarized Optical Microscopy (POM) Observation. The crystal morphology was observed through a POM (Axioskop40A Pol, Nikon, Japan) equipped with a λ plate ($\lambda = 530$ nm). Preparing 1 mm thick, thin films of composite material and PLA by the hot pressing method. The selected samples were kept at 250 °C for 3 min to eliminate heat history, and then isothermal at different temperatures (140, 130, and 120 °C) for 30 min. They were then held at room temperature for 8 h before undergoing polarizing microscope testing.

3. RESULTS AND DISCUSSION

3.1. Copolymer PESL Synthesis. In this study, SA, EG, and LA as primary starting materials were directly copolymerized in bulk through a two-step process involving esterification and polycondensation in the catalysis of TTP (Scheme 1). The resulting copolymers exhibited distinct ^1H NMR signals characteristic of the PES segments, as illustrated in Figure S1. An interesting observation was made regarding the proton signals a and c of the LA unit in the PESL copolymer, which showed a slight upfield shift in comparison to the signals from pure PLA. This shift suggested that a majority of the LA units were predominantly linked with SA or EG in the copolymer architecture. The resulting molar ratios (n_{LA}) of LA to SA in these copolymers were estimated by comparing the integral of the methyl group (c) in the PLA moieties to that of the carbonyl methylene (d) in the SA units. As the initial feeding molar ratio ($n_{\text{LA}0}$) of LA was increased from 30 to 70%, the characteristic signals (a and c) from the PLA segments gradually intensified, as depicted in Figure 1A. Compared to the characteristic peaks b and d of the PES segments, the proton signals b' and d' from the copolymers PESL52, PESL72, and PESL86 exhibited a pronounced downfield shift (Figure 1A). This was associated with SA and EG covalently binding LA. The same downfield shift of the methyl and methine signals from the LA units occurred as the LA content in the PESL copolymers increased from 20 to 86%, which indicated more PLA segments within the copolymer structure. Notably, the actual participation efficiency ($n_{\text{LA}}/n_{\text{LA}0}$) of the initial LA was less than 75% for PESL20 and PESL52 (20 and 52 represented the molar percentage content of LA units in the copolymers), as illustrated in Figure 1B. To enhance the utilization efficiency of LA, the esterification temperature was decreased to 190 °C, while maintaining the polycondensation temperature at 210 °C under a pressure of 20 Pa. As a result, $n_{\text{LA}}/n_{\text{LA}0}$ was significantly improved to 90% when the feeding ratio of LA relative to SA was set at 80% and 90%.

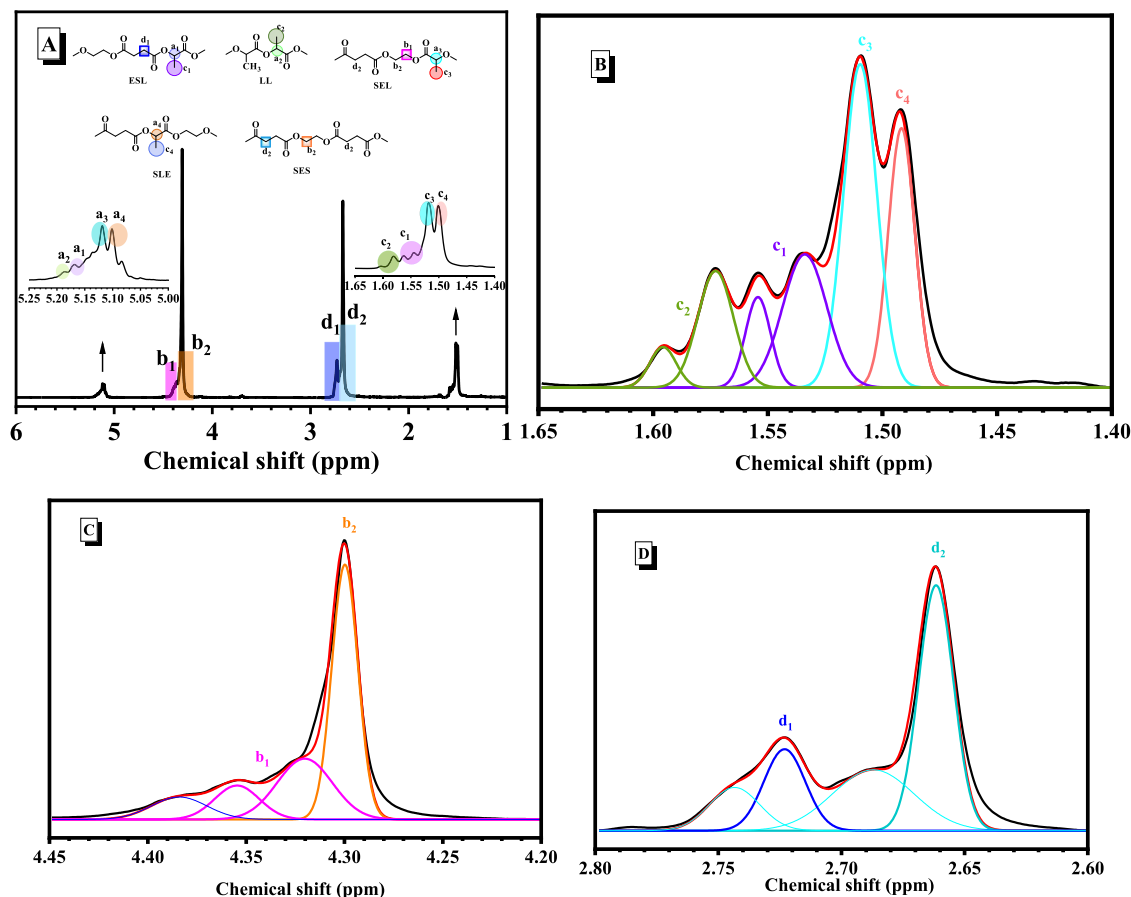


Figure 2. (A) Full spectrum of PESL52; (B–D) The regional ^1H NMR spectra of PESL52 were deconvoluted using Origin software. S stands for succinate unit, L represents lactate, and E means the ethylene glycol unit.

Table 1. Molecular Structures of PES and PESL Copolymers^a

sample	time ^d (h)	$n_{\text{LA}0}$ ^e (%)	n_{LA} ^f (%)	Y_{LL} ^g	Y_{ES} ^h	R ⁱ	$[\eta]$ ^j (dL/g)	GPC ^k		
								M_n (kDa)	M_w (kDa)	D
PES ^b	16						0.94	63	128	2.3
PESL20 ^b	4	30	20	1.2	1.6	1.45	0.89	53	96	1.8
PESL52 ^b	15	70	52	2.0	1.7	1.08	0.88	45	75	1.7
PESL72 ^c	16	80	72	2.8	1.6	0.99	0.79	37	61	1.7
PESL86 ^c	15	90	86	4.2	1.2	1.07	0.81	37	58	1.6

^aEsterification of SA and EG at the feeding molar ratio of 1–1.05 was carried out in the catalysis of TTP (the feed amount of TTP was 0.3 wt % of the total mass weight of SA and EG). ^bThe stages of esterification and polycondensation were performed at 210 and 240 °C, respectively. ^cThe stages of esterification and polycondensation were performed at 190 and 210 °C. ^dThe reaction time at the stage of polycondensation. ^eIndicating the feeding molar ratio of LA to SA. ^fThe actual molar content of LA in the resulting copolymers. ^gThe number-average sequence length of LA obtained by eq 1. ^hThe number-average sequence length of the PES block estimated by eq 2. ⁱRandom degree calculated by eq 3. ^jMeasured by Ubbelohde viscometer at 25 °C. ^kMeasured by GPC.

$$Y_{\text{LL}} = \frac{1}{3} \left(\frac{I_{c2} + I_{c1}}{I_{c1}} + \frac{I_{c2} + I_{c3}}{I_{c3}} + \frac{I_{c2} + I_{c4}}{I_{c4}} \right) \quad (1)$$

$$Y_{\text{ES}} = \frac{1}{2} \left(\frac{1/2 I_{b2} + I_{b1}}{I_{b1}} + \frac{1/2 I_{d2} + I_{d1}}{I_{d1}} \right) \quad (2)$$

$$R = (1/Y_{\text{LL}} + 1/Y_{\text{ES}}) \quad (3)$$

As referred,^{35,36} the regional ^1H NMR signals corresponding to the distinctive signals of PLA and PES components were deconvoluted using Origin software (see Figures 2 and S2–S4). This analysis was conducted to determine the average sequence lengths of the PLA and PES segments within the

copolymer's architecture. Figure 2A illustrates five possible regional linkage structures. The relative content fractions of the ESL, LL, SEL, and SLE segments were directly correlated with the integrals (I_{c1} , I_{c2} , I_{c3} , and I_{c4}) derived from the deconvoluted methyl signals of LA. The average sequence lengths of the LA segment, denoted as Y_{LL} , were calculated using eq 1 (Figure 2). Similarly, the average sequence length (Y_{PES}) of the PES segments was determined based on the proton signals b and d, as per eq 2. Y_{LL} and Y_{PES} remained consistently low regardless of variations in the LA feeding ratios (Table 1). The degree of randomness (R) for these copolymers, as determined by Y_{LL} and Y_{PES} (eq 3), was close to 1.0, indicating random copolymerization. The intrinsic

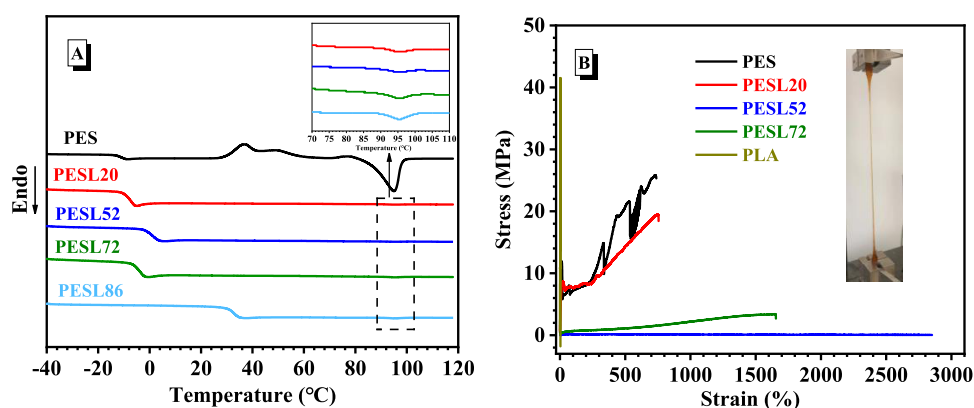


Figure 3. (A) DSC curves in the second heating; (B) Stress–strain curves of PES, pure PLA, and the copolymers PESL.

Table 2. Thermal and Mechanical Properties of the Copolymer PESL

sample	DSC		E (MPa)	σ_m (MPa)	ϵ_b (%)
	T_g (°C)	T_m (°C)			
PLA	58.0	159.2	2715.9 ± 508	39.9 ± 4.8	3.9 ± 1.7
PES	−11.9	94.8	248.0 ± 8.6	23.4 ± 4.9	642.0 ± 13.5
PESL20	−8.3	95.3	237.9 ± 9.1	8.0 ± 0.6	793.9 ± 67.0
PESL52	1.0	95.3	0.53 ± 0.07	0.15 ± 0.03	>1500
PESL72	−4.28	95.3	12.1 ± 2.0	3.12 ± 0.38	>1500
PESL86	32.7	95.3			

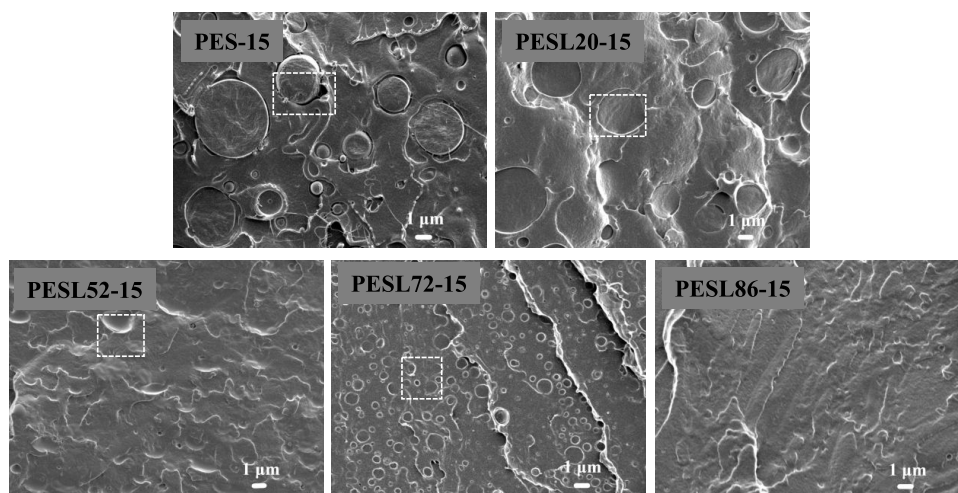


Figure 4. SEM images of cryo-fractured surfaces of blends: PES-15 stands for PES at a loading of 15 wt % blending with PLA.

viscosities of these copolymers were in the range of 0.8 and 0.9 dL/g, while their M_n values measured by GPC were controlled from 37 to 53 kDa.

3.2. Thermal Properties and Mechanical Behaviors of the Copolymer PESL. The thermal characteristics of the PESL copolymers were investigated by using differential scanning calorimetry (DSC). Compared to PES, the glass transition temperatures (T_g s) of these copolymers exhibited a notable increase from −8.33 to 32.74 °C with an increase in LA content (Figure 3A). A single faint melting peak at 95 °C was observed for each copolymer (inset in Figure 3A), indicating a quite low crystalline ability.

The mechanical properties of the PESL copolymers were evaluated at room temperature. The stress–strain curves depicted in Figure 3B revealed distinctive behaviors. PES exhibited a yielding point characteristic of semicrystalline

polymers. However, with the inclusion of the LA content, PESL20 displayed elastic deformation occurring at strains below 18%. After reaching a yield strength of 8.5 MPa, a noticeable decrease in stress was attributed to the motion of polymer segments, causing strain softening. The continuous application of stress induced significant material deformation, and the movement and alignment of segments led to strain hardening. This, in turn, increased the strength to 19 MPa with an elongation at break of $794 \pm 67\%$ (Table 2). As the LA content was increased to 52% in the resulting copolymers, the tensile strength experienced a rapid decline to 0.05 MPa, accompanied by the elongation at break exceeding 2000%, exhibiting impressive ductility. Conversely, PESL72 with a higher LA content showed strain hardening under continuous stress. PESL72 with a tensile strength of 3.12 MPa and an elongation at break over 1500% demonstrated its low strength

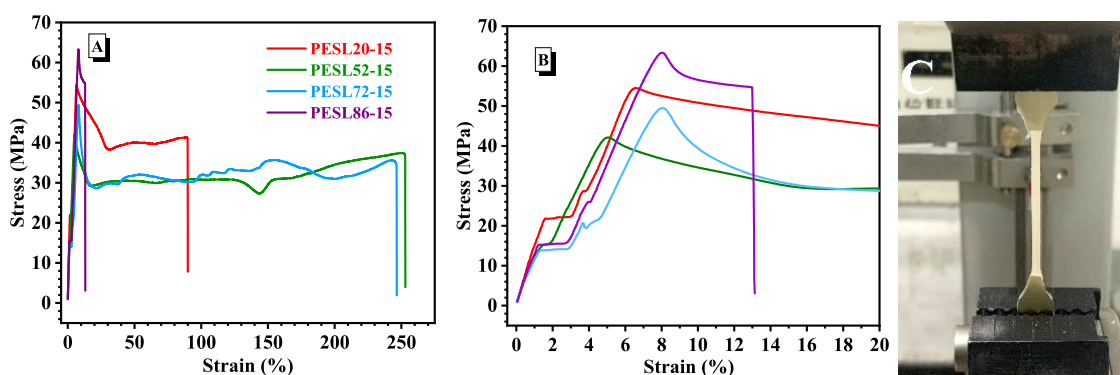


Figure 5. Tensile behavior of the blends with the copolymer PESL at a loading of 15 wt %. (A) Typical stress–strain curves for the blend films. (B) Regional scale-expanded curves for the strain within 20%. (C) Digital images recording the tension of the blend PESL72-15 during the tensile deformation until the generation of fracture. Plastic deformation-induced stress whitening was clearly observed for.

Table 3. Mechanical Properties of the Blends PESL/PLA, Pure PLA, and PES Blending with PLA

sample	E (MPa)	σ_m (MPa)	ϵ_b (%)	impact strength (kJ/m ²)
PES-15 ^a	2325.8 ± 455.4	25.7 ± 1.5	4.7 ± 0.2	27.2 ± 1.0
PESL20-15 ^b	3780.8 ± 83.6	54.4 ± 1.0	90.5 ± 30.7	20.7 ± 1.3
PESL52-15 ^b	2550.7 ± 588.8	40.8 ± 2.9	252.2 ± 4.0	12.2 ± 7.5
PESL72-15 ^b	3166.6 ± 176.8	49.0 ± 1.7	238.1 ± 11.9	18.2 ± 1.4
PESL86-15 ^b	3558.5 ± 138.6	60.7 ± 3.7	18.6 ± 12.4	12.3 ± 2.8
PLA	2715.9 ± 508	39.9 ± 4.8	3.9 ± 1.7	27.2 ± 1.0

^aStanding for PES at a loading of 15 wt % blending with PLA. ^bThe first number in the sample name means the LA content in the copolymers PESL; and the second number indicates the loading weight percentage of PESL in the blends.

and high flexibility and ductility (Figure 3B). Due to the random copolymerization and its low MW, the copolymer PESL86 was too brittle to make it for mechanical testing.

3.3. Copolymer PESL Blending with Pure PLA. Based upon the fundamental principles of toughening mechanisms, which primarily involve achieving a uniform dispersion and partial miscibility of the incorporated polymer within the PLA matrix,³⁷ these copolymers PESL at a loading of 15 wt % were blended with pure PLA ($M_n = 110$ kDa), respectively. The cryo-fractured surfaces of the resulting blends were measured by SEM observation (Figure 4). In comparison to neat PLA, which displayed a smooth and uniform surface,²⁹ the PES/PLA blends named by PES-15 (PES with a loading of 15 wt % in the blends) exhibited a sea–island morphology. The round PES phase particles were dispersed within the PLA matrix, indicating the immiscible nature of PLA and PES. The distinct gap observed between the dispersed PES and the PLA matrix signified poor interfacial adhesion and strong interfacial tension. Conversely, in the case of PLA/PESL blends, the shape and size of the dispersed phase underwent significant changes in morphology, and the gap between PLA and PESL was notably reduced. Particularly, the PESL52-15 blends (the copolymer PESL52 with a loading of 15 wt %) displayed no clear gap in the sea island, suggesting strong interfacial adhesion between PLA and PESL52. PESL72-15 blends exhibited smaller round dispersed phases than PESL20-15, suggesting the better compatibility between PESL72 and PLA. The blends PESL86-15 presented a relatively smooth surface without evident sea–island morphology, closely resembling pure PLA. This was attributed to the high content of LA units in the copolymer.

It is widely recognized that the mechanical properties of polymer blends are closely intertwined with their morphologies. Consequently, we conducted a comparative investigation

of the mechanical properties of PESL/PLA blends through tensile testing. Pure PLA, owing to its inherent brittleness, exhibited immediate fracture following elastic deformation at a low strain of 8% (Figure 3B). Similarly, for PLA/PES blends (PES-15) containing 15 wt % PES, rapid fracture occurred along with a meager elongation at break of 5% and an ultimate strength of approximately 25.7 MPa (Figure S6). This was associated with the immiscibility between the PES and PLA. Figure 5 illustrates a remarkable change from brittleness to ductility upon the copolymer PESL blending with pure PLA, and the mechanical properties of the blends were effectively tailored by varying the copolymer components. All of the blends exhibited high E and σ_m (Table 3 and Figure 5B). With the exception of PESL86-15 blends, strain hardening was observed in the other blends before catastrophic fracture, resulting in an ultimate strength of approximately 30 MPa. Consequently, substantial stress whitening was observed in the plastically deformed regions of PLA blends (Figure 5C) after surpassing the yield strength. This stress reduction during strain softening was primarily associated with the movement of blended segments. Under continuous stress, the incorporation of PESL into PLA led to a notable increase in the elongation at break for these blends. The mobility of the blending chains depended on the chemical components of the PESL copolymers. Notably, the PESL52-15 and PESL72-15 blends displayed an elongation at a break of 250% and an ultimate strength of 35 MPa. This enhanced toughness and ductility can be attributed to the improved miscibility of the two copolymers and pure PLA, supported by the SEM results. The good mechanical properties of PESL52-15 and PESL72-15 are of critical importance for expanding the use of PLA in packaging and other applications. Remarkably, when PESL86 was incorporated into PLA, the blends exhibited an elongation

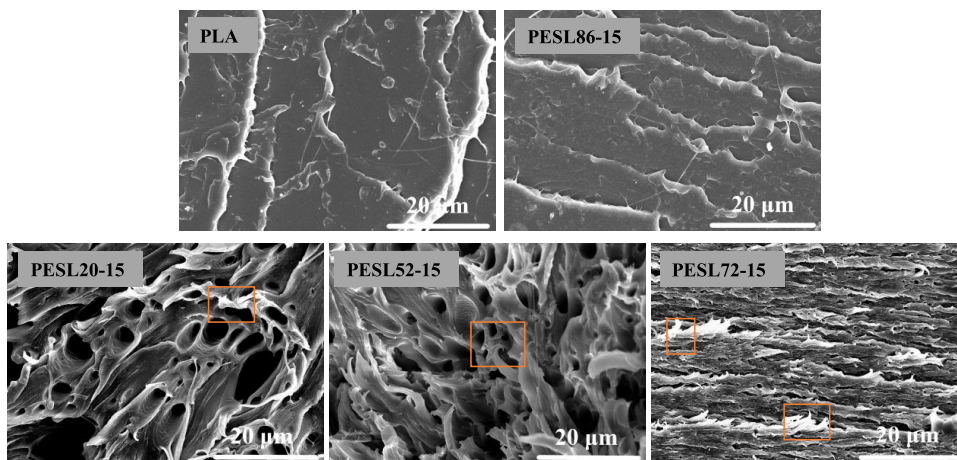


Figure 6. SEM micrographs of fracture surfaces after tensile failure for neat PLA and PESL/PLA blends.

at a break of only 13% with an ultimate strength of 54 MPa, indicative of their rigidity and brittleness.

The mechanical durability of PLA/PESL blends was further elucidated through the direct examination of their fracture surfaces following tensile failure. With the exception of PESL86-15 blends, which displayed a brittle deformation mode similar to neat PLA, the predominant mode of extension for PESL20-15, PESL52-15, and PESL72-15 was characterized by rubber-like plastic deformation (Figure 6). The variations in the chemical composition of the copolymers induced some disparities in plastic deformation. In these cases of PESL52-15 and PESL72-15, chain bundles underwent significant elongation, evolving into the ligaments adorned with distinctive worm-like wrinkles (marked in an orange square in Figure 6). This phenomenon highlighted the remarkable extensibility of PLA chains facilitated by the incorporation of the partially miscible PESL. The formation and growth of these worm-like wrinkles within the highly deformed substrate played a significant role in transferring and redistributing the applied stress load. This process, in turn, contributed significantly to the enhancement of the ductility and toughness of these blends.

Figure 7 displays the impact strength of each blend PLA/PESL sample performed with unnotched specimens (Figure S7). These blends showed an impact strength lower than that of neat PLA. The blend PESL52-15 had a low impact resistance ability, which is related to the low tensile strength of the copolymer PESL52 itself. The blend PLA/PESL72 with a good tensile property showed 18.4 kJ/m² of impact strength (Table 3).

3.4. Thermal Properties of the Blends. The thermal characteristics of PLA/PESL blends were comprehensively studied through DSC, TGA, and DMA. To assess the thermal stability of these blends, we examined the temperatures corresponding to 5% mass loss ($T_{5\%}$) and the peak decomposition rate (T_{\max}). As outlined in Figure 8A and summarized in Table 4, all of the blends exhibited a single thermal degradation stage within the measurement range, with slight variations in $T_{5\%}$ and T_{\max} depending on the chemical composition of PESL. Importantly, all of the initial decomposition temperatures exceeded 310 °C, underscoring their excellent thermal stability.

The impact of PESL copolymers on the molecular characteristics and phase transitions of PLA was unveiled

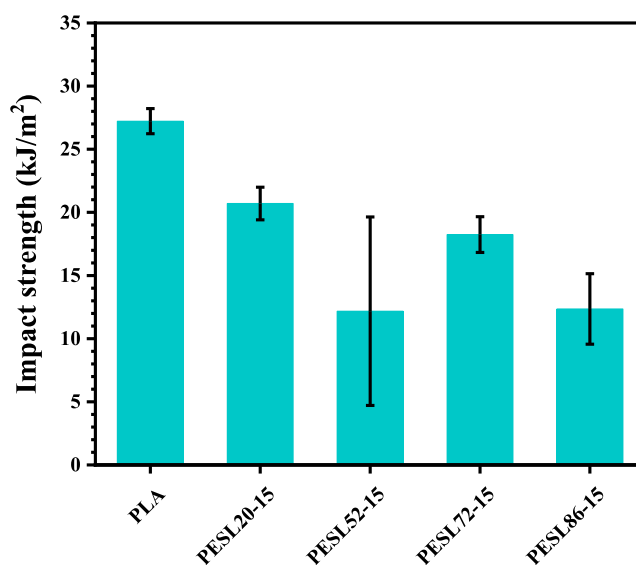


Figure 7. Impact strength of pure PLA and the blends PLA/PESL.

through a DSC analysis (Figure 8B). During the second heating cycle, in comparison to the T_g of 55 °C observed for pure PLA,³⁸ the T_g values for all the PLA/PESL blends exhibited a moderate decrease to around 50 °C. This reduction indicated that the inclusion of PESL with a lower T_g enhanced the chain mobility within the overall PLA matrix. The introduction of PESL copolymers, with improved chain mobility and the occurrence of heterogeneous nucleation preferentially at the interfaces between the PLA matrix and the dispersed microphase, resulted in a prominent cold crystallization phenomenon occurring at approximately 100 °C (T_{cc}) for the blends. This was in contrast to the less defined crystallization observed around 122 °C for pure PLA.³⁸ Additionally, the DSC analysis revealed a double-peak melting pattern for all of the blends, with peaks occurring at approximately 150 °C (T_{m1}) and 160 °C (T_{m2}). The lower T_{m1} , compared to the T_m of pure PLA, was likely due to the lamellar rearrangement during the melt-crystallization of PLA.³⁹ Conversely, T_{m2} indicated the preferential formation of ordered lamellae within the original crystals of the blends, contributing to their enhanced thermal stability.⁴⁰

Furthermore, direct POM observation of the isothermal crystalline morphology was conducted to investigate the

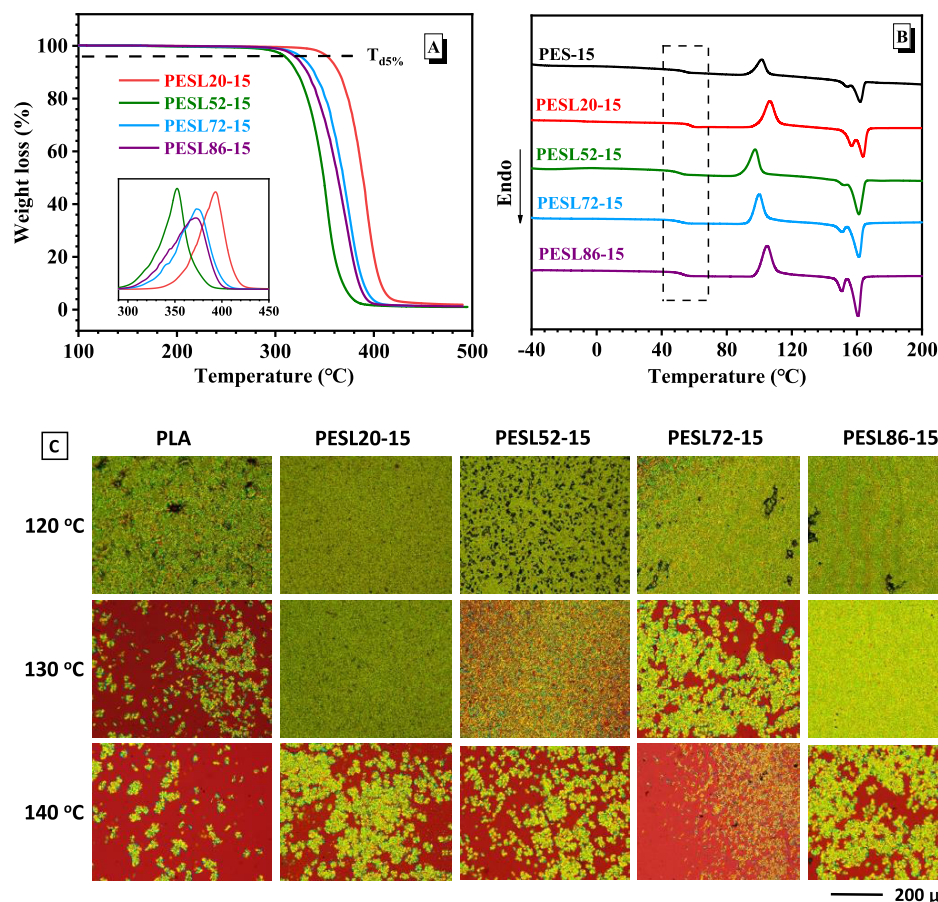


Figure 8. Thermal properties of PESL/PLA blends. (A) TGA curves, dTG curves in the inset; (B) DSC curves of the second heating scans; (C) POM images of isothermally crystallized blends after isothermal crystallization for 30 min. The scale bar denotes 200 μm for all images.

Table 4. Thermal Properties of Blending Polymers

sample	DSC				TGA		DMA	
	T_g ($^{\circ}\text{C}$)	T_m ($^{\circ}\text{C}$)	ΔH_m (J/g)	T_c ($^{\circ}\text{C}$)	$T_{d5\%}$ ($^{\circ}\text{C}$)	T_{dmax} ($^{\circ}\text{C}$)	T_{g1} ($^{\circ}\text{C}$)	T_{g2} ($^{\circ}\text{C}$)
PES-15	53.4	156.5	29.9	94.9	n.d.	n.d.	29.7	67.7
PESL20-15	57.6	158.7	27.9	99.9	355.5	393.4	-4.9	65.1
PESL52-15	51.2	154.7	33.3	97.0	312.5	352.4	-7.2	64.8
PESL72-15	51.8	156.8	28.6	94.4	328.9	372.9	-0.3	61.7
PESL86-15	53.1	155.7	29.7	98.7	322.8	372.4		65.4

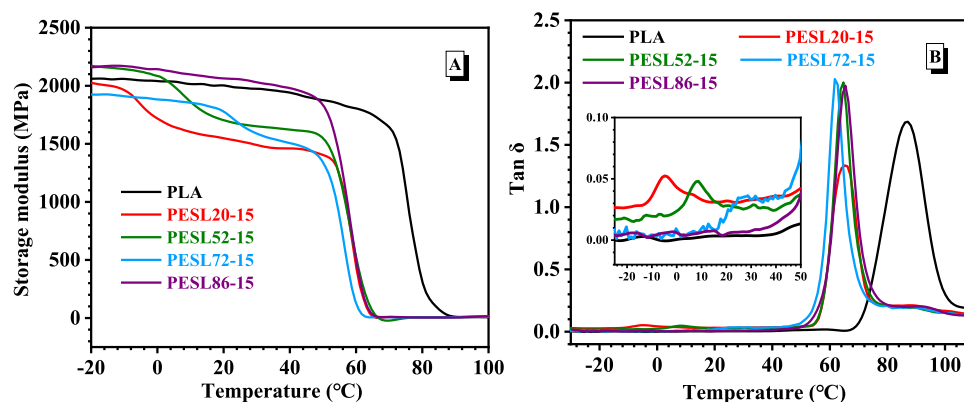


Figure 9. DMA results of the blends. (A) Storage modulus curves; (B) $\tan \delta$ as a function of temperature.

underlying crystallization state of PLA accelerated by PESL copolymers (Figure 8C). With the assistance of PESL

copolymers, the mobility of PLA chains was significantly enhanced, which was particularly beneficial for zone crystal-

lization. Consequently, the nucleation density of the blends was remarkably increased in comparison to that of neat PLA at the corresponding temperature.

In this study, DMA measurements were conducted to examine the thermomechanical properties of the PLA/PESL blends. The storage modulus (E') and $\tan \delta$ of the PLA/PESL blends as functions of temperature are illustrated in Figure 9. Compared to neat PLA, which displayed a rapid decrease in E' above 70 °C (Figure 9A), the E' curves for the blends PESL20-15, PESL52-15, and PESL72-15 exhibited a distinct two-stage drop within the measured temperature range. The E' values of these three blends gradually decreased as they were heated from -20 to 60 °C and then exhibited a sharp decrease above 60 °C. This phenomenon can be attributed to the highly elastic nature of the PESL copolymers, which reduced interactions between chains and segments within the PLA crystal region. Consequently, the E' values of these blends were slightly lower than that of pure PLA during heating.

The $\tan \delta$ peaks signify the relaxation temperatures of the polymers and correspond to the increased molecular mobility above the glass transition temperature. Consequently, these blends displayed two distinct $T_{g,s}$, with the lower one T_{g1} associated with the PESL component and the higher one T_{g2} attributed to the PLA component (Figure 9B). These dual relaxation behaviors suggest partial miscibility between PLA and the PESL copolymer. The PESL copolymers, known for their flexibility and low T_g values, served to enhance the flexibility of the blends, resulting in the production of flexible plastics. Notably, such T_{g1} shifted to higher temperatures as the LA content in the PESL copolymer increased from 20 to 86%, and it gradually weakened, indicating a slow dissipation of immiscibility. In the case of PESL86-15, the change in E' closely paralleled that of pure PLA upon heating, and its T_g value (65 °C) lower than neat PLA (86 °C) suggested an even higher level of flexibility. All of these results indicate that PLA properties can be effectively tuned by the incorporation of PESL-varying chemical component contents.

4. CONCLUSIONS

The copolymerization of SA, EG, and LA was executed to produce fully renewable PESL copolymers. When blending with PLA, it resulted in a robust interfacial adhesion between the PLA and PESL domains, primarily attributed to the enhanced interfacial compatibility facilitated by the LA components of the copolymers PESL. These structural characteristics bestowed the PLA blends with a unique combination of tensile toughness and strength, as vividly demonstrated by PESL52-15 and PESL72-15, exhibiting an elongation at a break of 250% and an ultimate strength of 35 MPa. The remarkable extension of PLA chains, brought about by the incorporation of partially miscible PESL copolymers, transformed them into resilient ligaments. These ligaments were proficient in transferring and redistributing the applied stress load. This convenient and cost-effective strategy presents a novel pathway for the development of functional packaging materials based on PLA, thereby opening up new possibilities in this field.

■ ASSOCIATED CONTENT

SI Supporting Information

The Supporting Information is available free of charge at <https://pubs.acs.org/doi/10.1021/acsomega.3c07489>.

S1: The full and regional ^1H NMR spectra of the copolymers PESL deconvoluted using Origin software. S2: DSC curve of neat PLA. S3: Typical stress–strain curve of PES/PLA blends. S4: Dimensions of unnotched specimens (PDF)

■ AUTHOR INFORMATION

Corresponding Author

Yinbiao Feng – State Key Laboratory of Chemical Resource Engineering, Beijing Key Laboratory of Bioprocess, College of Life Science and Technology, Beijing University of Chemical Technology, Beijing 100029, China; orcid.org/0000-0002-1832-9619; Email: yangj@mail.buct.edu.cn

Authors

Yinbiao Feng – State Key Laboratory of Chemical Resource Engineering, Beijing Key Laboratory of Bioprocess, College of Life Science and Technology, Beijing University of Chemical Technology, Beijing 100029, China

Cong Wang – State Key Laboratory of Chemical Resource Engineering, Beijing Key Laboratory of Bioprocess, College of Life Science and Technology, Beijing University of Chemical Technology, Beijing 100029, China

Junjiao Yang – College of Chemistry, Beijing University of Chemical Technology, Beijing 100029, China; orcid.org/0000-0003-3883-1566

Tianwei Tan – State Key Laboratory of Chemical Resource Engineering, Beijing Key Laboratory of Bioprocess, College of Life Science and Technology, Beijing University of Chemical Technology, Beijing 100029, China; orcid.org/0000-0001-5960-0009

Complete contact information is available at: <https://pubs.acs.org/10.1021/acsomega.3c07489>

Author Contributions

[§]Yinbiao Feng and Cong Wang contributed equally to this work. Ji.Y. contributed to conceptualization, supervision, writing. C.W. contributed to investigation and result analysis. Y.F. contributed to investigation and data curation. Ju.Y. contributed to SEM measurement. T.T. contributed to concept and funding acquisition

Notes

The authors declare no competing financial interest.

■ ACKNOWLEDGMENTS

This work was supported by Sponsored by Beijing Nova Program (No. 20220484165); Joint Project of BRC-BC (Biomedical Translational Engineering Research Center of BUCT-CJFH) (XK2023-13).

■ REFERENCES

- (1) Inkinen, S.; Hakkarainen, M.; Albertsson, A.-C.; Södergård, A. From lactic acid to poly(lactic acid) (PLA): characterization and analysis of PLA and its precursors. *Biomacromolecules* **2011**, *12*, 523–532.
- (2) Yu, J.; Xu, S.; Liu, B.; Wang, H.; Qiao, F.; Ren, X.; Wei, Q. PLA Bioplastic production: from monomer to the polymer. *Eur. Polym. J.* **2023**, *193*, No. 112076.
- (3) Abdelshafy, A.; Hermann, A.; Herres-Pawlis, S.; Walther, G. Opportunities and challenges of establishing a regional bio-based polylactic acid supply chain. *Global Challenge* **2023**, *7*, No. 2200218.

- (4) Wang, Z.; Ganewatta, M. S.; Tang, C. Sustainable polymers from biomass: bridging chemistry with materials and processing. *Prog. Polym. Sci.* **2020**, *101*, No. 101197.
- (5) Slomkowski, S.; Penczek, S.; Duda, A. Poly lactides—an overview. *Polym. Adv. Technol.* **2014**, *25*, 436–447.
- (6) Haider, T. P.; Völker, C.; Kramm, J.; Landfester, K.; Wurm, F. R. Plastics of the future? the impact of biodegradable polymers on the environment and on society. *Angew. Chem., Int. Ed.* **2019**, *58*, 50–62.
- (7) Schneiderman, D. K.; Hillmyer, M. A. 50th anniversary perspective: there is a great future in sustainable polymers. *Macromolecules* **2017**, *50*, 3733–3749.
- (8) Liu, H.; Zhang, J. Research progress in toughening modification of poly (lactic acid). *J. Polym. Sci., Part B: Polym. Phys.* **2011**, *49*, 1051–1083.
- (9) Yang, X.-M.; Qiu, S.; Yusuf, A.; Sun, J.; Zhai, Z.; Zhao, J.; Yin, G.-Z. Recent advances in flame retardant and mechanical properties of polylactic acid: a review. *Int. J. Biol. Macromol.* **2023**, *243*, No. 125050.
- (10) Ali, W.; Ali, H.; Gillani, S.; Zinck, P.; Souissi, S. Polylactic acid synthesis, biodegradability, conversion to microplastics and toxicity: a review. *Environ. Chem. Lett.* **2023**, *21*, 1761–1786.
- (11) Aversa, C.; Barletta, M.; Cappiello, G.; Gisario, A. Compatibilization strategies and analysis of morphological features of poly (butylene adipate-co-terephthalate) (PBAT)/poly(lactic acid) PLA blends: a state-of-art review. *Eur. Polym. J.* **2022**, *173*, No. 111304.
- (12) Krishnan, S.; Pandey, P.; Mohanty, S.; Nayak, S. K. Toughening of polylactic acid: an overview of research progress. *Polym.-Plast. Technol. Eng.* **2016**, *55*, 1623–1652.
- (13) Liu, H.; Zhang, J. Research progress in toughening modification of poly (lactic acid). *J. Polym. Sci., Part B: Polym. Phys.* **2011**, *49*, 1051–1083.
- (14) Zhao, X.; Hu, H.; Wang, X.; Yu, X.; Zhou, W.; Peng, S. Super tough poly (lactic acid) blends: a comprehensive review. *RSC Adv.* **2020**, *10*, 13316–13368.
- (15) Nofar, M.; Salehiyan, R.; Ciftci, U.; Jalali, A.; Durmus, A. Ductility improvements of PLA-based binary and ternary blends with controlled morphology using PBAT, PBSA, and nanoclay. *Compos. Part B* **2020**, *182*, No. 107661.
- (16) Anderson, K.; Schreck, K.; Hillmyer, M. Toughening polylactide. *Polym. Rev.* **2008**, *48*, 85–108.
- (17) Rasal, R. M.; Janorkar, A. V.; Hirt, D. E. Poly (lactic acid) modifications. *Prog. Polym. Sci.* **2010**, *35*, 338–356.
- (18) Yang, Y.; Zhang, L.; Xiong, Z.; Tang, Z.; Zhang, R.; Zhu, J. Research progress in the heat resistance, toughening and filling modification of PLA. *Sci. China: Chem.* **2016**, *59*, 1355–1368.
- (19) Cheng, Y. L.; Deng, S. B.; Chen, P.; Ruan, R. Polylactic acid (PLA) synthesis and modifications: a review. *Front. Chem. China* **2009**, *4*, 259–264.
- (20) Liu, H. Z.; Zhang, J. W. Research progress in toughening modification of poly (lactic acid). *J. Polym. Sci., Part B: Polym. Phys.* **2011**, *49*, 1051–1083.
- (21) Su, S.; Kopitzky, R.; Tolga, S.; Kabasci, S. Polylactide (PLA) and its blends with poly (butylene succinate) (PBS): a brief review. *Polymers* **2019**, *11*, 1193.
- (22) Ding, Y.; Lu, B.; Wang, P. L.; Wang, G.; Ji, J. H. PLA-PBAT-PLA tri-block copolymers: effective compatibilizers for promotion of the mechanical and rheological properties of PLA/PBAT blends. *Polym. Degrad. Stab.* **2018**, *147*, 41–48.
- (23) Ostafinska, A.; Fortelný, I.; Hodan, J.; Krejčíková, S.; Nevalová, M.; Kredatusová, J.; Kruliš, Z.; Kotek, J.; Šlouf, M. Strong synergistic effects in PLA/PCL blends: Impact of PLA matrix viscosity. *J. Mech. Behav. Biomed. Mater.* **2017**, *69*, 229–241.
- (24) Ding, Y.; Feng, W.; Huang, D.; Lu, B.; Wang, P.; Wang, G.; Ji, J. Compatibilization of Immiscible PLA-based biodegradable polymer blends using amphiphilic di-block copolymers. *Eur. Polym. J.* **2019**, *118*, 45–52.
- (25) Liu, T.-Y.; Lin, W.-C.; Yang, M.-C.; Chen, S.-Y. Miscibility, thermal characterization and crystallization of poly (L-lactide) and poly(tetramethylene adipate-co-terephthalate) blend membranes. *Polymer* **2005**, *46*, 12586–12594.
- (26) Sangeetha, V. H.; Deka, H.; Varghese, T. O.; Nayak, S. K. State of the art and future prospectives of poly (lactic acid) based blends and composites. *Polym. Compos.* **2018**, *39*, 81–101.
- (27) Yu, L.; Dean, K.; Li, L. Polymer blends and composites from renewable resources. *Prog. Polym. Sci.* **2006**, *31*, 576–602.
- (28) Lim, L. T.; Auras, R.; Rubino, M. Processing technologies for poly (lactic acid). *Prog. Polym. Sci.* **2008**, *33*, 820–852.
- (29) Xu, H.; Zhou, J.; Odelius, K.; Guo, Z.; Guan, X.; Hakkarainen, M. Nanostructured phase morphology of a biobased copolymer for tough and UV-resistant polylactide. *ACS Appl. Polym. Mater.* **2021**, *3*, 1973–1982.
- (30) Bai, Z.; Liu, Y.; Su, T.; Wang, Z. Effect of hydroxyl monomers on the enzymatic degradation of poly (ethylene succinate), poly (butylene succinate) and poly (hexylene succinate). *Polymers* **2018**, *10*, No. 90.
- (31) Qiu, S.; Zhang, K.; Su, Z.; Qiu, Z. Thermal behavior, mechanical and rheological properties, and hydrolytic degradation of novel branched biodegradable poly (ethylene succinate) copolymers. *Polym. Test.* **2018**, *66*, 64–69.
- (32) Zhang, K.-J.; Qiu, Z. Miscibility and crystallization behavior of novel branched poly (ethylene succinate)/poly (vinyl phenol) blends. *Chin. J. Polym. Sci.* **2019**, *37*, 1169–1175.
- (33) Gan, Z.; Abe, H.; Doi, Y. Biodegradable poly (ethylene succinate) (PES). I. crystal growth kinetics and morphology. *Biomacromolecules* **2000**, *1*, 704–712.
- (34) Papageorgiou, G. Z.; Bikiaris, N. D. Crystallization and melting behavior of three biodegradable poly (alkylene succinates). a comparative study. *Polymer* **2005**, *46*, 12081–12092.
- (35) Li, J.; Jiang, Z.-Q.; Zhou, J.; Liu, J.; Shi, W.-T.; Gu, Q.; Wang, Y.-Z. A novel aromatic-aliphatic copolyester of poly (ethylene-co-diethylene terephthalate)-co-poly (L-lactic acid): synthesis and characterization. *Ind. Eng. Chem. Res.* **2010**, *49*, 9803–9810.
- (36) Hu, H.; Zhang, R.; Shi, L.; Ying, W. B.; Wang, J.; Zhu, J. Modification of poly (butylene 2,5-furandicarboxylate) with lactic acid for biodegradable copolyesters with good mechanical and barrier properties. *Ind. Eng. Chem. Res.* **2018**, *57*, 11020–11030.
- (37) Si, W.-J.; Yang, L.; Zhu, J.; Li, Y.-D.; Zeng, J.-B. Highly toughened and heat-resistant poly (L-lactide) materials through interfacial interaction control via chemical structure of biodegradable elastomer. *Appl. Surf. Sci.* **2019**, *483*, 1090–1100.
- (38) Mauck, S. C.; Wang, S.; Ding, W.; Rohde, B. J.; Fortune, C. K.; Yang, G.; Ahn, S.-K.; Robertson, M. L. Biorenewable tough blends of polylactide and acrylated epoxidized soybean oil compatibilized by a polylactide star polymer. *Macromolecules* **2016**, *49*, 1605–1615.
- (39) Xu, J.-Z.; Chen, T.; Yang, C.-L.; Li, Z.-M.; Mao, Y.-M.; Zeng, B.-Q.; Hsiao, B. S. Isothermal crystallization of poly (L-lactide) induced by graphene nanosheets and carbon nanotubes: a comparative study. *Macromolecules* **2010**, *43*, 5000–5008.
- (40) Xie, L.; Sun, X.; Tian, Y.; Dong, F.; He, M.; Xiong, Zheng, Y. Q. Self-nanofibrillation strategy to an unusual combination of strength and toughness for poly (lactic acid). *RSC Adv.* **2017**, *7*, 11373–11380.